Chemical Physics Letters 462 (2008) 238–242

Contents lists available at ScienceDirect

Chemical Physics Letters

journal homepage: www.elsevier.com/locate/cplett

Vibrational dynamics of benzoic acid in nonpolar solvents studied by subpicosecond infrared pump–probe spectroscopy

Sayuri Yamaguchi [a], Motohiro Banno [b], Kaoru Ohta [a], Keisuke Tominaga [a,b,c,*], Tomoyuki Hayashi [d]

[a] Graduate School of Science and Technology, Kobe University, Nada, Kobe, 657-8501, Japan
[b] Molecular Photoscience Research Center, Kobe University, Nada, Kobe, 657-8501, Japan
[c] CREST/JST, Molecular Photoscience Research Center, Kobe University, Nada, Kobe 657-8501, Japan
[d] Chemistry Department, University of California, Irvine, Irvine, CA 92697-2025, USA

ARTICLE INFO

Article history:
Received 17 May 2008
In final form 29 July 2008
Available online 6 August 2008

ABSTRACT

The vibrational dynamics of the OH stretching mode of the benzoic acid dimer in nonpolar solvents have been studied by subpicosecond, frequency-resolved infrared pump–probe spectroscopy. The signal consists of biexponential decay and a quantum beat, which is due to the intermolecular mode of the hydrogen bond coupled to the OH stretching mode. The subpicosecond component is suggested to be due to the vibrational relaxation of the low-frequency modes of the dimer, whereas the picosecond component is assigned to vibrational cooling. The frequency of the Fourier spectra of a quantum beat correlates with that of the OH stretching mode. The physical origin of the correlation is discussed.

1. Introduction

The strength of hydrogen bonds is generally between those of covalent bonds and intermolecular interactions such as van der Waals force. This 'intermediate' nature of hydrogen bonds results in various chemical and biological events [1–3]. For example, biological macromolecules such as nucleic acids and proteins often express and control their functions by rearranging their hydrogen bonds. To deepen our understanding of hydrogen bonds, it is necessary to investigate intermolecular vibrations of hydrogen-bonded complexes.

Carboxylic acids in solutions are important model systems for studying hydrogen bonds [4–6]. Benzoic acid (BA) is a carboxylic acid and forms dimers or complexes with solvent molecules in various solutions [7]. Intermolecular hydrogen bonds of these complexes markedly affect the dynamics of intramolecular vibrational modes associated with hydrogen bonds. The OH stretching mode is a good probe for investigating the microscopic environment around the oscillator of hydrogen-bonded complexes. The effects of hydrogen bonds on the dynamics of the OH stretching mode in the vibrationally excited state have been extensively studied by time-resolved vibrational spectroscopy [8–20].

To understand the mechanism of the vibrational dynamics of the intramolecular mode such as vibrational energy relaxation, the anharmonic coupling between the intra- and intermolecular vibrational modes should be considered. Recently, two-dimensional vibrational spectroscopy, a vibrational analogue of two-dimensional NMR spectroscopy, has been proven useful for investigating the anharmonic coupling between intramolecular modes [21–26]. This powerful technique has not yet been applied to studies of the coupling between the intramolecular and intermolecular modes.

Recently, Heyne and coworkers have studied the anharmonic coupling between the OH stretching and intermolecular low-frequency modes of the acetic acid dimer by analyzing the quantum beat observed in infrared (IR) pump–probe signals [8–15]. More recently, they have extended their work to the 7-azaindole dimer [16,17]. In this work, we study the vibrational energy relaxation of the OH stretching mode of the BA complex in nonpolar solvents by frequency-resolved IR pump–probe spectroscopy. In particular, we focus on the dependence of the frequency of the intermolecular mode on probe frequency.

2. Experimental

BA-d_5 and solvents (i.e., CCl_4, $CDCl_3$, and C_6D_6) from Sigma–Aldrich were used without further purification. Details of the subpicosecond IR pump–probe spectroscopy are described elsewhere [27]. Briefly, we obtained IR pulses by difference frequency mixing with signal and idler pulses in the near-IR region generated by a home-built optical parametric amplifier. The pulse duration of the IR pulse was approximately 200 fs. We split the IR pulse into pump, probe, and reference pulses, and the probe and reference pulses were detected by an array detector after passing through a monochromator. The samples were contained in a cell with an optical path length of 0.5 mm. The optical density at the excitation wavenumber was approximately 0.6.

* Corresponding author. Address: Graduate School of Science and Technology, Kobe University, Nada, Kobe, 657-8501, Japan.
E-mail address: tominaga@kobe-u.ac.jp (K. Tominaga).

0009-2614/$ - see front matter © 2008 Published by Elsevier B.V.
doi:10.1016/j.cplett.2008.07.108

3. Density functional calculation

We performed the normal-mode frequency calculation of the BA dimer with the density functional theory (DFT) at the B3LYP/6-31++G(d,p) level using GAUSSIAN 03. The results are summarized in Table 1. We also obtained cubic anharmonicities as described previously [28–30]. The potential energy V of the BA dimer was expanded around the equilibrium geometry to a quartic order in four relevant normal coordinates (Q_1: dimer in-plane bending mode, Q_2: dimer stretching mode, Q_3: in-phase OH stretching mode, Q_4: out-of-phase OH stretching mode). The potential energy is expressed as

$$V = \frac{1}{2}\sum_{i}^{4} f_{ii}Q_i^2 + \frac{1}{6}\sum_{i,j,k}^{4} f_{ijk}Q_iQ_jQ_k + \frac{1}{24}\sum_{i,j,k,l}^{4} f_{ijkl}Q_iQ_jQ_kQ_l \quad (1)$$

with the nth-order force constants given by

$$f_{ijk\cdots} = \left(\frac{\partial^n V}{\partial Q_i \partial Q_j \partial Q_k \cdots}\right)_{\mathrm{eq}} \quad (2)$$

where $(\,)_{\mathrm{eq}}$ represents the derivatives taken at the equilibrium geometry. The cubic and quartic anharmonic force constants were determined numerically by computing the first and second derivatives of the analytical quadratic force constants with 3-point central difference formulas. The results are summarized in Table 2 together with those reported for the acetic acid dimer obtained by the same calculation method [13].

4. Results and discussion

Fig. 1 shows the solvent dependence of the IR spectra of the OH stretching mode of BA-d_5. The peak wavenumber is located at approximately 3000 cm^{-1}, and the spectra show a broad band with complicated structures. From the dependence of the IR spectrum on the concentration of BA in CCl_4 (0.5–100 mM), the broad band at approximately 3000 cm^{-1} is assigned to a cyclic dimer of BA, which is consistent with results of the previous work [7]. The structures in the spectrum result from the intermolecular vibrations within the dimer, the Fermi resonance, and the Davydov coupling [8,31,32]. The spectra of the three solutions are identical. Therefore, we conclude that BA exists as a cyclic dimer in $CDCl_3$ and C_6D_6.

Table 1
Harmonic frequencies of the normal modes of benzoic acid dimer calculated by the DFT and their assignment

Frequency (cm^{-1})	Approximate description[a]
19.0	'Butterfly'
31.2	Torsion ('twist')
58.8	Cogwheel
62.9	τ(Ph–COOH) twisting
71.5	τ(Ph–COOH) twisting
88.4	τ(–COOH)
106.7	H-Bond shearing (dimer in-plane bending)
112.9	ν_s(O···O) (dimer stretching)

[a] The assignment is followed by Boczar et al. [34]. ν, Stretching; τ, torsion.

Table 2
Cubic anharmonicities of benzoic acid dimer and acetic acid dimer[a]

ijk	f_{ijk}[a] Benzoic acid dimer	f_{ijk}[a,b] Acetic acid dimer
114	0.00	–
144	53.78	151
224	0.00	–
244	−202.98	−145

Mode 1 is the dimer in-plane bending mode, mode 2 is the dimer stretching mode, and mode 4 is the OH stretching mode.
[a] Unit is cm^{-1}.
[b] From Ref. [13].

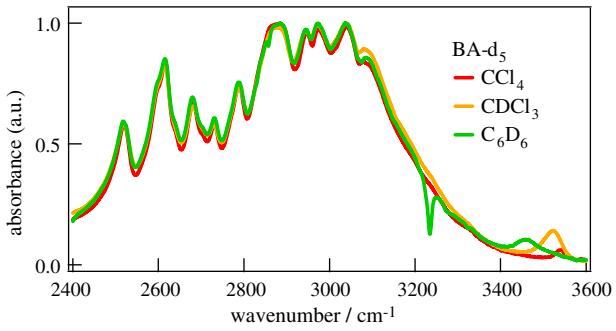

Fig. 1. Absorption spectra of the OH stretching mode. The solvents are indicated in the inset.

Fig. 2 shows a frequency-resolved pump–probe signal of the OH stretching mode of BA-d_5 in CCl_4. The pump and probe pulses have a central wavenumber at 3000 cm^{-1}. Fig. 3 shows the time profiles of the signal at 2840 cm^{-1}, 3000 cm^{-1} and 3124 cm^{-1}. A similar time evolution including a quantum beat was observed in the pump–probe signal of the acetic acid dimer [8,9]. This quantum beat was interpreted to be due to the coupling with the low-frequency intermolecular mode of hydrogen bonds, considering the selection rule of the transition based on the symmetry of the dimer [8,13].

To investigate the quantum beat and incoherent decay separately, we fit the signal after a delay time of 0.3 ps because a coherent artifact due to pulse overlapping contaminates the signal at approximately $t = 0$. All the signals show a double exponential feature. The time constants of the incoherent signal are 730 ± 70 fs and 13 ± 2 ps at 3000 cm^{-1}. At 3124 cm^{-1}, the signal turns to a transient absorption component instantaneously after the excitation, which is followed by decay on the picosecond time scale. The vibrational excitation energy of the OH stretching mode dissipates into the environment around the oscillator, and this transient absorption component on the higher-frequency side results from a blue shift of the spectrum in the vibrational ground state caused by local heating. Therefore, we conclude that the vibrational population relaxation of the OH stretching mode takes place within our time resolution (<200 fs). For a deuterated acetic acid dimer ($(CD_3COOH)_2$), Heyne et al. observed the decay of the vibrationally excited state of the OH stretching mode and obtained a vibrational energy relaxation time of 200 fs [13].

The time constants of the picosecond component are 13 ± 2 ps, 13 ± 4 ps, and 6 ± 2 ps for CCl_4, $CDCl_3$, and C_6D_6, respectively. This component corresponds to vibrational cooling, and the time

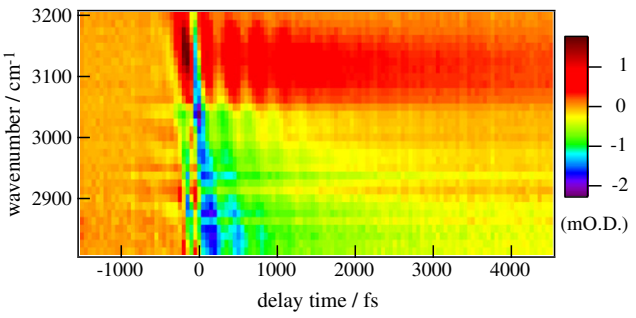

Fig. 2. Frequency-resolved pump–probe signal of the OH stretching mode of 120 mM BA-d_5 in CCl_4.

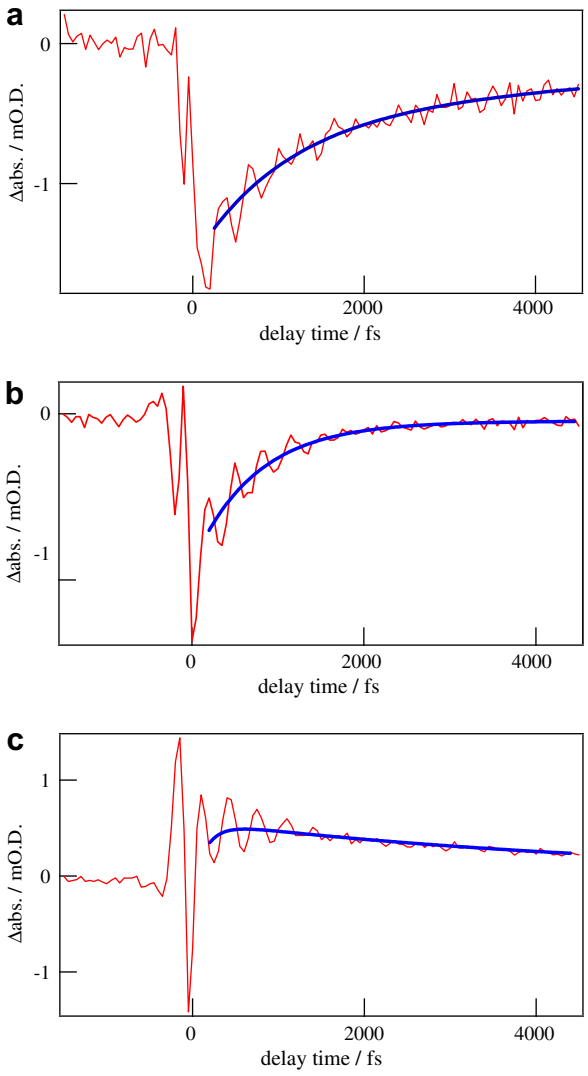

Fig. 3. Pump–probe signals of the OH stretching mode of 120 mM BA-d_5 in CCl_4 at 2840 cm^{-1} (a), 3000 cm^{-1} (b), and 3124 cm^{-1} (c). Blue curves are the results of fitting using a double exponential function. (For interpretation of the references to colour in this figure legend, the reader is referred to the web version of this article.)

constant correlates well to the thermal conductivity of the solvent; that is 104 k, 117 k, and 144 k (k = mW m^{-1} K^{-1}) for CCl_4, $CDCl_3$, and C_6D_6, respectively [33]. The subpicosecond component could be due to vibrational energy relaxation (VER) of the low-frequency modes of the BA dimer. The excitation energy of the OH stretching mode dissipates into the lower-frequency modes within 200 fs after the excitation, and the low-frequency modes of the dimer complex may be excited on the subpicosecond time scale. In this state, the vibrational population of all the modes of the BA dimer may not yet reach the Boltzmann distribution. Subsequently, it reaches the thermal distribution by the VER of these modes and/or the dissipation of energy into the solvent occurring simultaneously. Interestingly, the subpicosecond component depends on excitation wavenumber. For example, the subpicosecond time constants are 1.5 ± 0.4 ps, 1.5 ± 0.2 ps, and 730 ± 70 fs at 2725 cm^{-1}, 2788 cm^{-1}, and 3000 cm^{-1}, respectively. For the acetic acid dimer, Heyne et al. also observed a similar nonexponential cooling with time constants of 1.5 ps and 15 ps [13].

We conclude that the quantum beat results from the ground state of the OH stretching mode from the following consideration. As discussed by Heyne et al., the quantum beat is due to intermolecular modes anharmonically coupled to the OH stretching mode. The vibrational coherence of these intermolecular modes is generated in both the excited and ground states of the OH stretching mode by IR excitation. Since the lifetime of the excited state is less than 200 fs, the population in the excited state is transferred to the ground state immediately after excitation. The vibrational coherence of the intermolecular mode may be transferred to the higher vibrational states of these modes in the ground state of the intramolecular mode ($v_{OH} = 0$), which is followed by the VER of the intermolecular modes. However, it is unlikely that this coherence transfer occurs, because the frequency of the quantum beat does not change during observation; the observed signal can be reproduced well by the function $\exp(-t/\tau)\cos(\omega t + \phi)$ at a delay time between 0.3 ps and 1.5 ps, as shown in Fig. 4. If the quantum beat comes from the higher vibrational states of the low-frequency intermolecular modes, we would expect to observe a frequency change in this time region because the intermolecular mode is strongly anharmonic in general. Therefore, we conclude that the low-frequency intermolecular mode is in its ground state ($v_{LF} = 0$) when the quantum beat is observed; consequently, the quantum beat represents the coherence between the $v_{LF} = 0$ and 1 states. Since the energy of the low-frequency mode is on the order of the thermal energy, the population of this mode is partially excited to the higher vibrational states. Therefore, the Fourier spectrum of the quantum beat is a thermal average of the mode weighted by the Boltzmann distribution. Note that the higher excited states of the low-frequency modes in the $v_{OH} = 0$ state may contribute to the incoherent signal, and the subpicosecond component in the pump–probe signal may be the VER of the low-frequency modes, as described earlier.

We analyzed the quantum beat in the pump–probe signals of the BA dimer by Fourier-transforming the oscillatory part. By subtracting the fitting results with double exponential decay from the observed signal, we obtained an oscillatory part of the signal. Fig. 5a shows the Fourier spectrum of the oscillation at a probe wavenumber of 3124 cm^{-1}, and Fig. 5b shows a two-dimensional map of the Fourier spectra of the quantum beat and the probe wavenumber. A single band is observed at approximately 105 cm^{-1}. According to the DFT calculation, there are two normal modes at approximately 105 cm^{-1} for the BA dimer: the dimer stretching mode at 112.9 cm^{-1} and the in-plane bending mode at 106.7 cm^{-1}. The calculation of these low-frequency modes has been reported and the results are similar to the previous results [34,35]. Heyne et al. observed two low-frequency modes at 145 cm^{-1} and 170 cm^{-1} in the Fourier spectra of the quantum beat of the acetic acid dimer $(CH_3COOD)_2$. By comparing the results obtained by the DFT calculation, they assigned the bands at 145 cm^{-1} and 170 cm^{-1} to the dimer stretching and dimer in-plane bending

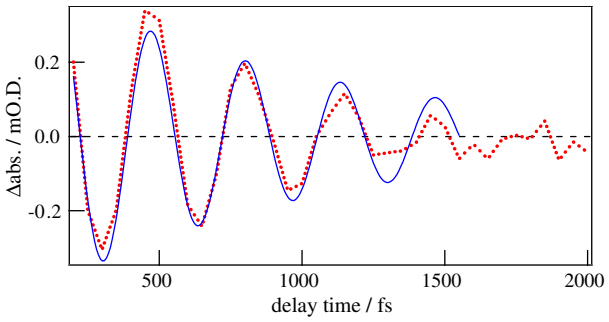

Fig. 4. Oscillatory component of the pump–probe signal at 3124 cm^{-1}. Blue line is a result of the fitting using the function $\exp(-t/\tau\cos(\omega t + \phi)$. (For interpretation of the references to color in this figure legend, the reader is referred to the web version of this article.)

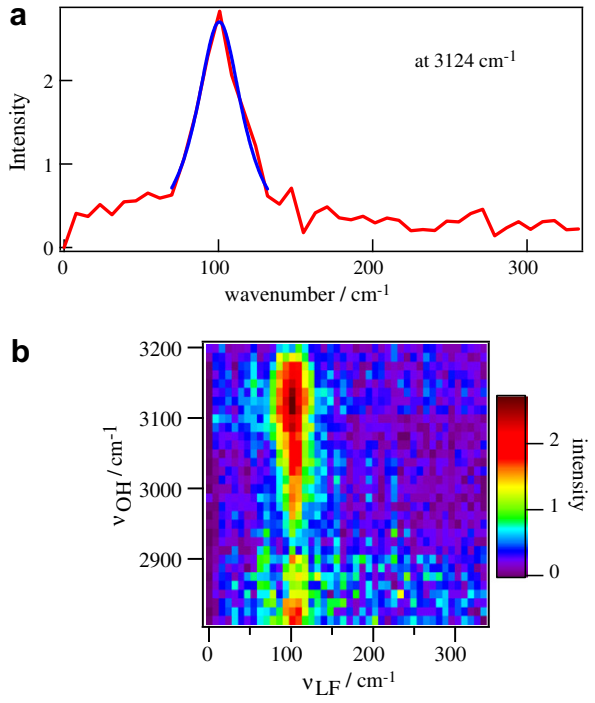

Fig. 5. Fourier spectrum of the quantum beat at 3124 cm^{-1} and fit by Lorentzian (blue line). (a) 2D map of Fourier spectra in the entire probe wavenumber region. (b) ν_{LF} and ν_{OH} denote the frequencies of the low-frequency mode and OH stretching mode, respectively. (For interpretation of the references to color in this figure legend, the reader is referred to the web version of this article.)

modes, respectively [8,13]. At a certain probe wavenumber (2250 cm^{-1}), a third band is also observed at 45 cm^{-1}. Interestingly, note that the relative intensities of the two bands (namely, the dimer stretching and in-plane bending modes) depend on probe wavenumber [9].

To obtain the peak wavenumber of the low-frequency mode more accurately, we fitted the Fourier spectra with a Lorentzian function (Fig. 5a). The results are shown in Fig. 6. The error bar of the peak frequency estimated from the spectral fitting is less than 1 cm^{-1}. In the figure, we show the three experimental results

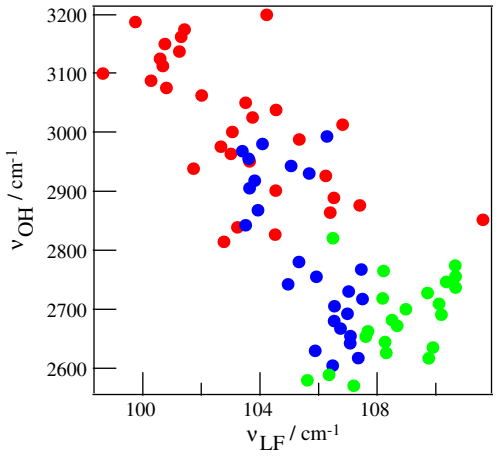

Fig. 6. Dependence of the low-frequency mode (ν_{LF}) on the probe wavenumber of the OH stretching mode (ν_{OH}). Colored dots correspond to results of the experiment with a different central wavenumber of excitation; red: 3000 cm^{-1}, blue: 2800 cm^{-1}, and green: 2700 cm^{-1}. (For interpretation of the references to color in this figure legend, the reader is referred to the web version of this article.)

obtained at different central wavenumbers of excitation: 2700 cm^{-1} (green points), 2800 cm^{-1} (blue points), and 3000 cm^{-1} (red points). Although the points are somewhat scattered, it is clear that the peak wavenumber of the low-frequency mode depends on the frequency of the OH stretching mode; that is, as the frequency of the OH stretching mode increases, the low-frequency mode shifts to the lower-frequency side. By least-squares fitting, we obtained $\nu_{LF} = -0.013 \times \nu_{OH} + 142$, where ν_{LF} and ν_{OH} are the wavenumbers of the low-frequency and OH stretching modes, respectively. We also obtained the correlation diagrams of other less polar solvents, namely, C_6D_6 and $CDCl_3$, and a similar dependence of the low-frequency mode on the OH stretching mode is observed (data not shown here). Thus, such a dependence is generally observed for the BA dimer in solution.

We next discuss the possible origins of this dependence. First, Fermi resonance may contribute to oscillation. However, as discussed in detail by Heyne et al., oscillation due to Fermi resonance should disappear within a dephasing time between the $v = 0$ and $v = 1$ states of the OH stretching mode [13]. In this case, the lifetime of the vibrationally excited state is shorter than the time resolution, which is less than 200 fs. Since the dephasing (T_2) should be smaller than twice the population relaxation time (T_1), it is unlikely that the Fermi resonance would contribute to the observed quantum beat.

Second, the overlap of the two spectra may affect the central frequency of the Fourier spectrum. Since the two intermolecular modes have resonance frequencies near 105 cm^{-1} for the BA dimer, the effective central frequency may change if the coupling strength of these modes depends on probe wavenumber. Actually, Heyne et al. observed two coupled low-frequency modes at 145 cm^{-1} and 175 cm^{-1}, whose relative intensities in the Fourier spectrum change as functions of probe wavenumber. The DFT calculation of the cubic anharmonicity for the BA dimer, however, shows that the dimer stretching mode couples with the OH stretching mode much stronger than with the in-plane bending mode. This result is in sharp contrast to that in the case of the acetic acid dimer in which the cubic anharmonicities of the two modes are of the same order. For the 7-azaindole dimer, the cubic anharmonicity between the dimer stretching mode and the NH stretching mode is predominant, similarly to that for benzoic acid dimer. Therefore, we conclude that a single low-frequency mode contributes to the Fourier spectrum of the BA dimer.

Finally, an inhomogeneous distribution of hydrogen bond strength could result in the correlation between the OH stretching and low-frequency intermolecular modes. Since the higher-frequency side of the OH stretching mode corresponds to weaker hydrogen-bonding dimers, the low-frequency intermolecular mode may depend on hydrogen bond strength; note that weakly hydrogen-bonding complexes exhibit higher-frequency OH stretching modes and lower-frequency dimer stretching modes. In solution, such an inhomogeneous distribution could arise if the dimer structure depends on the microscopic environment around the dimer. However, this interpretation is valid only when the band is inhomogeneously broadened. The existence of structures in the IR spectrum suggests that the band is homogeneously broadened. However, the existence of structures in the IR spectrum does not necessarily mean that the bandwidth is predominated by a homogeneous contribution. If the band of the dark state that interacts with the OH stretching mode by Fermi resonance is homogeneously broadened, the resulting band may show structures even if the OH stretching mode is inhomogeneous. The key question is how large the inhomogeneity is for the OH stretching band, which can be clarified by IR photon echo and two-dimensional IR spectroscopies.

In summary, we studied the vibrational dynamics of the OH stretching mode of the benzoic acid dimer in nonpolar solvents

by frequency-resolved IR pump–probe spectroscopy. The pump–probe signal shows biexponential decay as well as a quantum beat. The slow component of the biexponential decay is vibrational cooling, probably corresponding to thermal diffusion in the solvent. The origin of the fast component is not clear yet; however, the vibrational energy relaxation of the low-frequency modes has been proposed as a possible candidate for its origin. The Fourier spectra of the quantum beat show a single band at approximately 105 cm^{-1}. Comparing the results with those of the DFT calculation, we assigned this low-frequency band to the dimer stretching mode, which is anharmonically coupled to the OH stretching mode. Interestingly, we observed a correlation between the low-frequency intermolecular and OH stretching modes. An inhomogeneous distribution of hydrogen bond strength could be the origin of this correlation.

References

[1] G.A. Jeffrey, An Introduction to Hydrogen Bonding, Oxford University Press, 1997.
[2] G.R. Desiraju, T. Steiner, The Weak Hydrogen Bond, Oxford University Press, 1998.
[3] G.C. Pimentel, A.L. McClellan, The Hydrogen Bond, Reinhold Publishing Corporation, 1960.
[4] Y. Maréchal, A. Witkowski, J. Chem. Phys. 48 (1968) 3697.
[5] M. Wójcik, Mol. Phys. 36 (1978) 1757.
[6] Y. Maréchal, J. Chem. Phys. 87 (1987) 6344.
[7] P. Novak, D. Vikić-Topić, Z. Meić, S. Sekušak, A. Sablijić, J. Mol. Struct. 356 (1995) 131.
[8] E.T.J. Nibbering, T. Elsaesser, Chem. Rev. 104 (2004) 1887.
[9] K. Heyne, N. Huse, E.T.J. Nibbering, T. Elsaesser, Chem. Phys. Lett. 369 (2003) 591.
[10] K. Heyne, N. Huse, E.T.J. Nibbering, T. Elsaesser, J. Phys.: Condens. Matter 15 (2003) S129.
[11] N. Huse, K. Heyne, J. Dreyer, E.T.J. Nibbering, T. Elsaesser, Phys. Rev. Lett. 91 (2003) 197401.
[12] T. Elsaesser, N. Huse, J. Dreyer, J.R. Dwyer, K. Heyne, E.T.J. Nibbering, Chem. Phys. 91 (2003) 197401.
[13] K. Heyne, N. Huse, J. Dreyer, E.T.J. Nibbering, T. Elsaesser, J. Chem. Phys. 121 (2004) 902.
[14] N. Huse, B.D. Bruner, M.L. Cowan, J. Dreyer, E.T.J. Nibbering, R.J.D. Miller, T. Elsaesser, Phys. Rev. Lett. 95 (2005) 147402.
[15] J. Dreyer, J. Chem. Phys. 122 (2005) 184306.
[16] J.R. Dwyer, J. Dreyer, E.T.J. Nibbering, T. Elsaesser, Chem. Phys. Lett. 432 (2006) 146.
[17] J. Dreyer, J. Chem. Phys. 127 (2007) 054309.
[18] R. Laenen, C. Rauscher, A. Laubereau, Chem. Phys. Lett. 283 (1998) 7.
[19] H.J. Bakker, Chem. Rev. 108 (2008) 1456.
[20] K. Ohta, K. Tominaga, Chem. Phys. 341 (2007) 310.
[21] R.M. Hochstrasser, Proc. Natl. Acad. Sci. USA 104 (2007) 14190.
[22] J. Bredenbeck, J. Helbing, C. Kolano, P. Hamm, Chem. Phys. Chem. 8 (2007) 1747.
[23] M. Khalil, N. Demirdöven, A. Tokmakoff, J. Phys. Chem. A 107 (2003) 5258.
[24] S. Park, K. Kwak, M.D. Fayer, Laser Phys. Lett. 10 (2007) 704.
[25] D. Abrabavicius, S. Mukamel, Chem. Phys. 318 (2005) 50.
[26] M. Cho, Chem. Rev. 108 (2008) 1331.
[27] M. Banno, K. Ohta, K. Tominaga, J. Phys. Chem. A 112 (2008) 4170.
[28] T. Hayashi, S. Mukamel, Bull. Korean Chem. Soc. 24 (2003) 1097.
[29] T. Hayashi, S. Mukamel, J. Phys. Chem. A 107 (2003) 9113.
[30] W. Schneider, W. Thiel, Chem. Phys. Lett. 157 (1989) 367.
[31] D. Chamma, O. Henri-Rousseau, Chem. Phys. 248 (1999) 53.
[32] D. Chamma, O. Henri-Rousseau, Chem. Phys. 248 (1999) 71.
[33] Y.S. Tououkian et al., Thermophysical Properties of Matter, Plenum Press, 1970, vol. III.
[34] M. Boczar, K. Szczeponek, M.J. Wójcik, C. Paluszkiewicz, J. Mol. Struct. 700 (2004) 39.
[35] J. Antony, G. von Helden, G. Meijer, B. Schmidt, J. Chem. Phys. 123 (2005) 014305.